Actin-dependent Mitochondrial Motility in Mitotic Yeast and Cell-Free Systems: Identification of A Motor Activity on the Mitochondrial Surface

Viviana R. Simon, Theresa C. Swayne, and Liza A. Pon

Department of Anatomy and Cell Biology, College of Physicians and Surgeons, Columbia University, New York 10032

Abstract. Using fluorescent membrane potential sensing dyes to stain budding yeast, mitochondria are resolved as tubular organelles aligned in radial arrays that converge at the bud neck. Time-lapse fluorescence microscopy reveals region-specific, directed mitochondrial movement during polarized yeast cell growth and mitotic cell division. Mitochondria in the central region of the mother cell move linearly towards the bud, traverse the bud neck, and progress towards the bud tip at an average velocity of 49 ± 21 nm/sec. In contrast, mitochondria in the peripheral region of the mother cell and at the bud tip display significantly less movement. Yeast strains containing temperature sensitive lethal mutations in the actin gene show abnormal mitochondrial distribution. No mitochondrial movement is evident in these mutants after short-term shift to semipermissive temperatures. Thus, the actin cytoskeleton is important for normal mitochondrial movement during inheritance. To determine the possible role of known myosin genes in yeast mitochondrial motility, we investigated mitochondrial inheritance in *myo1, myo2, myo3* and *myo4* single mutants and in a *myo2, myo4* double mutant. Mitochondrial spatial arrangement and motility are not significantly affected by these mutations. We used a microfilament sliding assay to examine motor activity on isolated yeast mitochondria. Rhodamine-phalloidin labeled yeast actin filaments bind to immobilized yeast mitochondria, as well as unilamellar, right-side-out, sealed mitochondrial outer membrane vesicles. In the presence of low levels of ATP (0.1–100 μM), we observe F-actin sliding on immobilized yeast mitochondria. In the presence of high levels of ATP (500 μM–2 mM), bound filaments are released from mitochondria and mitochondrial outer membranes. The maximum velocity of mitochondria-driven microfilament sliding (23 ± 11 nm/sec) is similar to that of mitochondrial movement in living cells. This motor activity requires hydrolysis of ATP, does not require cytosolic extracts, is sensitive to protease treatment, and displays an ATP concentration dependence similar to that of members of the myosin family of actin-based motors. This is the first demonstration of an actin-based motor activity in a defined organelle population.

MITOCHONDRIAL inheritance is the process whereby mitochondria are transferred from mother cells to developing daughter cells during cell division. In the budding yeast, *Saccharomyces cerevisiae*, this process begins at the G_1/S boundary of the cell division cycle (Stevens, 1981). Since mitochondria are produced only from preexisting mitochondria (Criddle and Schatz, 1969; Schatz and Saltzgaber, 1969), this inheritance process ensures that each daughter cell contains this indispensable organelle. We used budding yeast to study the dynamics of mitochondrial movements leading to inheritance, and the organelle-cytoskeletal interactions that control these movements.

Cell division in *S. cerevisiae* proceeds by asymmetric growth of the developing daughter cell. In yeast and other eukaryotes, the cytoskeleton is required for establishment of cell polarity. During yeast cell division, the microtubule cytoskeleton is required for spindle formation, chromosome segregation and nuclear migration into the bud (Jacobs et al., 1988; Huffaker et al., 1988). The yeast actin cytoskeleton consists of actin patches and actin cables. Actin patches are F-actin associated invaginations in the plasma membrane (Mulholland et al., 1994); actin cables consist of bundles of actin filaments. During asymmetric cell growth, actin patches accumulate at the site of bud emergence, inside the bud, and at the site of cell–cell separation. Actin cables are deposited as radial fibers that extend from the bud into deep within the mother cell (Adams and Pringle, 1984; Kilmartin and Adams, 1984). Phenotypic analysis of mutants defective in actin and actin-associated proteins implicate the actin cytoskeleton in several aspects of yeast cell function including endocytosis, mating projection formation, and nuclear migration during mating (Read et al., 1992; Kübler and Riezman, 1993). During cell division, the

Please address all correspondence to L. A. Pon, Department of Anatomy and Cell Biology, Columbia University, P&S 12-425, 630 West 168th Street, New York, NY 10032. Tel.: (212) 305-1947. Fax: (212) 305-3970.

actin cytoskeleton is required for bud site selection, polarized vesicle movement leading to bud growth, spindle alignment, cytokinesis, and septation (Adams and Pringle, 1984; Kilmartin and Adams, 1984; Novick and Botstein, 1985; Palmer et al., 1992; Johnston et al., 1991; Drubin et al., 1993).

Several findings indicate that transfer of mitochondria into buds is linked to the actin cytoskeletal component of the cell polarization machinery. Light microscopy studies reveal colocalization of mitochondria and actin cables (Drubin et al., 1993; Lazzarino et al., 1994). In addition, sedimentation assays demonstrate ATP-sensitive, reversible binding of isolated yeast mitochondria to F-actin. This binding is mediated by a protein or proteins on the mitochondrial surface and is blocked by pretreatment of F-actin with subfragment-1 from myosin (Lazzarino et al., 1994). In mutants bearing conditional lethal mutations in the major actin gene, *ACT1*, mitochondrial spatial arrangement and inheritance are impaired (Drubin et al., 1993; Lazzarino et al., 1994; Smith, M. G., V. R. Simon, L. A. Pon, manuscript submitted for publication). The mutant alleles used in this study include *act1-3*, which contains a P32L substitution, and *act1-133*, which contains two amino acid substitutions (D24A and D25A) within the myosin-binding site (Shortle et al., 1984; Kabsch et al., 1990; Wertman et al., 1992; Schröder et al., 1993; Rayment et al., 1993). At permissive temperatures (22°C) both mutants are viable but display poor actin cable formation, low growth rates, elevated levels of isotropic (nonpolarized) cell growth, and random bud site selection (Novick and Botstein, 1985; Drubin et al., 1993). Short term incubation at semipermissive (30°C) or nonpermissive (37°C) temperature results in mitochondrial aggregation. In addition, temperature-dependent inhibition of mitochondrial transfer from mother cell to bud occurs in the *act1-3* mutant. These findings suggest that mitochondria interact directly with the actin cytoskeleton, and that this interaction controls mitochondrial position and inheritance.

Actin-dependent movement of organelles and vesicles has been observed in *Acanthamoeba, Chara, Dictyostelium*, cultured fibroblasts and squid axon (Kachar, 1985; Adams and Pollard, 1986; Kachar and Reese, 1988; Wessels et al., 1989; Hegmann et al., 1990; Kuznetsov et al., 1992). The current model proposes that myosins, a family of actin-dependent motor molecules, bind to both microfilaments and organelles and use the energy of ATP hydrolysis to drive organelle movement along actin tracks (Adams and Pollard, 1989). This model is based on evidence that: (*a*) muscle and nonmuscle myosins display ATP-dependent motor activity (Sheetz and Spudich, 1983; Albanesi et al., 1985); (*b*) vesicles and organelles that bind to or move along F-actin contain proteins that are immunologically cross-reactive with myosin (Grolig et al., 1988; Fath and Burgess, 1993); and (*c*) anti-myosin antibodies and mutations of myosin genes inhibit actin-dependent particle movement in whole cells and cell-free systems (Adams and Pollard, 1986; Wessels and Soll, 1990; Johnston et al., 1991; Govindan et al., 1995).

At present, four myosin genes have been identified in *Saccharomyces cerevisiae*. The *MYO1* gene encodes a conventional, type II myosin. Mutant cells lacking this gene display lowered growth rates, delayed cytokinesis and defects in chitin deposition and cell wall formation (Watts et al., 1987; Rodriguez and Paterson, 1990). The *MYO2* gene is essential and encodes a calmodulin-associated type V myosin. Myo2p is localized to the bud neck and bud tip and has been implicated in post-Golgi transport of secretory vesicles during bud enlargement (Prendergast et al., 1990; Johnston et al., 1991; Brockerhoff et al., 1994; Lillie and Brown, 1994; Govindan et al., 1995). *MYO3* and *MYO4* encode type I and V myosins, respectively. Since deletion of these genes has no detectable phenotype, the function of these myosins is not known (Goodson et al., 1995; Haarer et al., 1994).

To examine the role of the actin cytoskeleton in mitochondrial inheritance in mitotic yeast, we (*a*) evaluated mitochondrial movements in living yeast; (*b*) determined the effect of mutations in the *ACT1, MYO1, MYO2, MYO3,* and *MYO4* genes on mitochondrial movements; and (*c*) used an in vitro motility assay to characterize an actin-dependent motor activity on the surface of isolated yeast mitochondria. Our studies demonstrate that yeast mitochondria interact directly with the actin cytoskeleton, and that mitochondrial movements during cell division are actin-mediated, regulated events. In addition, we have identified an actin-dependent motor activity on the mitochondrial outer membrane.

Materials and Methods

Yeast Cell Manipulation

Yeast cell growth, mating, sporulation, and other manipulations were carried out according to Sherman (1991).

Visualization of Mitochondria in Mitotic Yeast In Vivo

Yeast cells were grown to mid-log phase in rich medium containing glucose (YPD)[1] at 22°C. Cell density was adjusted to 10^7 cells/ml. Mitochondria were stained by incubating living cells with YPD medium containing the membrane potential-sensing dye, MitoTracker (10–20 nM; Molecular Probes, Eugene, OR) for 15 min at RT. In some experiments, mitochondria were stained by incubation in YPD containing 20 ng/ml of the membrane potential-sensing dye 3,3′-dihexyloxacarbocyanine iodide ($DiOC_6$; Molecular Probes) for 5 min at RT. Cells were then washed once and resuspended to a final concentration of 2×10^8 cells/ml in YPD medium. Samples were mounted on microscope slides and visualized by fluorescence microscopy as described below.

Preparation of Mitochondria, Mitochondrial Outer Membranes, and Actin from Yeast

Actin was isolated from mid-log phase yeast by DNaseI affinity chromatography and multiple rounds of polymerization and depolymerization as described previously (Lazzarino et al., 1994). Highly purified mitochondria were isolated from D27310B yeast by differential and isopycnic centrifugation using Nycodenz gradients as previously described (Lazzarino et al., 1994; Glick and Pon, 1995). Right-side-out, sealed, unilamellar mitochondrial outer membrane vesicles were isolated according to Riezman et al. (1983). Briefly, crude mitochondria were disrupted by hypotonic treatment followed by sonication. Membrane vesicles were isolated and concentrated by ultracentrifugation, and mitochondrial outer membrane vesicles were separated from other submitochondrial membrane particles by sucrose gradient centrifugation. Mitochondria and mitochondrial outer membrane vesicles were stored in aliquots in liquid nitrogen, and were thawed immediately before use.

1. *Abbreviations used in this paper*: OM, outer membrane; YPD, 1% yeast extract, 2% bactopeptone, 2% dextrose.

Table I. Yeast Strains Used in This Study

Strain	Genotype	Reference
D27310B	MATa	ATCC25657
MSY106	MATa/MATα, *his4-619/his4-619*	This laboratory
MSY202	MATa/MATα, *his4-619/his4-619, act1-3/act1-3*	This laboratory
DDY437	MATa/MATα, *ura3-52/ura3-52, his3Δ200/his3Δ200,ADE2/ade2, tub2-201/tub-201, leu2-3,112/leu2-3,112, ade4/ADE4, act1-133::HIS3/act1-133::HIS3*	D. Drubin
DBY745	MATα, *leu2-3,112, ura3-52, ade1-101*	J. Rodriguez-Medina
BN4	MATα, *leu2-3,112, ura3-52, ade1-101, myo1Δ::URA3*	J. Rodriguez-Medina
SLY87	MATa/MATα, *ura3-52/ura3-52, leu2-3,112/leu2-3,112, his4/his4, trp1-289/TRP1*	S. Brown
SLY88	MATa/MATα, *myo2-66/myo2-66, ura3/ura3, leu2/leu2, trp1Δ1/TRP1, his6/HIS6, his3/HIS3*	S. Brown
CRY3	MATa/MATα, *can1-100/can1-100, ade2-1/ade2-1, his3-11/his3-11, leu2-3,112/leu2-3,112, ura3-1/ura3-1*	J. Spudich
HGA1	MATa/MATα, *can1-100/can1-100, ade2-1/ade2-1, his3-11/his3-11, leu2-3,112/leu2-3,112, trp1-1/trp1-1, ura3-1/ura3-1, myo3::HIS3/myo3::HIS3*	J. Spudich
22AB	MATa/MATα, *lys2-80(am)/lys2-80(am), ura3-52/ura3-52, his3Δ200/his3Δ200, trp1-1(am)/trp1-1(am), leu2-3,112/leu2-3,112*	S. Brown
MYO4ΔU5	MATa/MATα, *lys2-80(am)/lys2-80(am), ura3-52/ura3-52, his3Δ200/his3Δ200, trp1-1(am)/trp1-1(am), leu2-3, 112/leu2-3,112, myo4::URA3/myo4::URA3*	S. Brown
VSY30	MATa/MATα, *leu2/leu2, myo2-66/myo2-66, myo4::URA3/myo4::URA3*	This Study

In Vitro Actin Binding and Motility Assay

We used a modification of the in vitro motility assay developed by Kron and Spudich (1986). The experimental flow cell consists of a nitrocellulose-coated (Fullam Inc., Latham, NY) coverslip placed on a microscope slide. Two parallel strips of double-sided tape are used as spacers to create a 35–50-μl flow chamber between the coverslip and the microscope slide. Mitochondria were suspended to a final concentration of 1 mg/ml in complete AB buffer (25 mM imidazole hydrochloride, pH 7.4, 25 mM KCl, 4 mM $MgCl_2$, 1 mM EGTA, 10 mM DTT, containing a protease inhibitors cocktail, 1 mM phenylmethy-sulfonyl fluoride, 10 μM benzamidine, 1 μg/ml 1,10-phenanthroline, 0.5 μg/ml antipain, 0.5 μg/ml chymostatin, 0.5 μg/ml leupeptin, 0.5 μg/ml pepstatin, and 0.5 μg/ml aprotinin (Sigma Chemical Co., St. Louis, MO); and oxygen scavengers, 3 mg/ml glucose, 9.3 U/ml glucose oxidase (Sigma Chemical Co.), 18 μg/ml catalase (Calbiochem, La Jolla, CA)). $DiOC_6$ (100 ng/ml) was added, and the suspension was perfused into the microscope flow cell. After incubation for 10 min at 4°C, the flow cell was washed with 3 vol of complete AB/BSA buffer (complete AB buffer containing 4 mg/ml BSA) and nonspecific protein binding sites were blocked by incubation with the AB/BSA buffer for 10 min at 4°C.

Rhodamine-phalloidin–labeled yeast actin filaments (1.5 μg/ml in complete AB buffer) were perfused into the flow cell and incubated with immobilized mitochondria for 10 min at RT. Unbound material was removed by three washes with AB buffer and mitochondria-microfilament complexes were visualized using fluorescence microscopy as described below. Microfilament sliding and release were observed after addition of AB buffer containing different concentrations of ATP (100 nM–2 mM) and an ATP regeneration system (10 μM creatine phosphate and 250 μg/ml creatine phosphokinase; Sigma Chemical Co.).

Analysis of F-actin binding to mitochondrial outer membrane vesicles was carried out using vesicle suspensions at a concentration of 1 mg/ml in complete AB buffer. For immobilization, microscope flow cells were perfused two times with the 1 mg/ml outer membrane solution; each perfusion was followed by a 10-min incubation at 4°C. All other manipulations were carried out as described above.

Trypsin pretreatment of mitochondria or mitochondrial outer membrane vesicles was carried out within the microscope flow cell. Mitochondria or outer membrane vesicles were incubated with 500 μg/ml or 125 μg/ml of trypsin (Sigma Chemical Co.), respectively, in protease inhibitor-free AB buffer for 10 min at 4°C. After treatment, samples were washed three times with AB buffer containing oxygen scavengers, protease inhibitors and soybean trypsin inhibitor (1 mg/ml; Sigma Chemical Co.).

Fluorescence Microscopy

Cells were viewed with a Leitz Dialux microscope (Rockleigh, NJ). MitoTracker-stained cells and rhodamine-phalloidin–labeled actin filaments were viewed with excitation and emission wavelengths of 540–552 nm and 570 nm, respectively. $DiOC_6$-stained cells and purified mitochondria were viewed with excitation and emission wavelengths of 490–495 nm and 525 nm, respectively. DAPI images were viewed with excitation and emission wavelengths of 340–365 nm and 450–488 nm, respectively. Images of stained mitochondria in whole cells were collected for 1–2 s at 20-s intervals. Images of microfilaments bound to immobilized mitochondria in vitro were collected for 5 s at 20-s intervals. In both cases, images were collected using a cooled CCD camera (Star-1, Photometrics, Tucson, AZ). Light output from the 100W Mercury Arc lamp was controlled using a shutter driver (Uniblitz D122, Vincent Associates, Rochester, NY) and attenuated using neutral density filters (Omega Optical Corporation, Brattleboro, VT). Image enhancement and analysis were performed on a Macintosh Quadra 800 computer (Cupertino, CA) using the public domain program NIH Image 1.55. Images were stored on a magnetic optical disk drive (Peripheral Land Inc., Fremont, CA).

Velocity Measurements

The velocities of mitochondrial movement in living cells and actin filament sliding on immobilized mitochondria were determined by measuring the change in position of the tip of each moving mitochondrion or actin filament as a function of time in time-lapse series. Sliding actin filaments were defined as filaments which (*a*) colocalized with immobilized mitochondria, (*b*) moved parallel to their long axis, and (*c*) displayed detectable, linear motion for 60 s of real time (three consecutive still frames). For whole cell studies, motile mitochondria were defined as particles which displayed linear, detectable movement for at least 60 s of real time. The limit of resolution of our system is 1 pixel/20 s or ~5.5 nm/sec. Mitochondrial or F-actin movements which resulted in displacement less than 1 pixel, or which persisted for less than three consecutive still frames, were assigned a velocity of 0 nm/sec.

Velocity measurements were determined by following the leading tip or trailing tail of the tubular mitochondria. Since >90% of the motile mitochondria displayed movements parallel to the long axis of the tubular organelle, rare lateral motions were interpreted as organelles moving into or out of the plane of focus and were not measured. Immobilization of the organelles in the cortex of mother cells was evident in cases where entire organelles were visible within one plane of focus, and no net change in position was detected. NIH Image was used to determine the position (x-y coordinates) of mitochondria and actin filaments. The linear distances between successive positions of mitochondria or microfilaments were calculated using Microsoft Excel, and instantaneous velocities were averaged to give the mean velocity.

Results

Mitochondrial Movements Leading to Organelle Inheritance

At low concentrations, the membrane potential sensing dyes $DiOC_6$ and MitoTracker preferentially stain mitochondria without affecting organelle size, position or shape

(Chen, 1989; Whitaker et al., 1991; Koning et al., 1993; Smith, M. G., V. R. Simon, and L. A. Pon, manuscript submitted for publication). These dyes, combined with time-lapse video microscopy, reveal a defined spatial arrangement and motility pattern of mitochondria in dividing yeast. In the mother cell, motile mitochondria are resolved as long tubular structures that form radial arrays and converge at the bud neck (Fig. 1, *A–C*). These mitochondria undergo linear movements that are parallel to the long axis of the tubular organelle (Fig. 1, *A–C*). The average velocity of mitochondrial movement is 49 ± 21 nm/sec (Fig. 2).

Mitochondrial movement during cell division is polarized. Organelles move from the central region of the mother cell toward the bud neck. Although several mitochondria move toward the bud simultaneously, the bud neck is a bottleneck: only one or two mitochondria enter the bud at any one time. Within the bud, organelles move from the neck toward the bud tip, where they accumulate (Fig. 1, *D–F*). The majority of motile mitochondria display this pattern of polarized movement: over 83% of the organelles evaluated in the central region of the mother cell, bud neck, and bud move toward the bud tip.

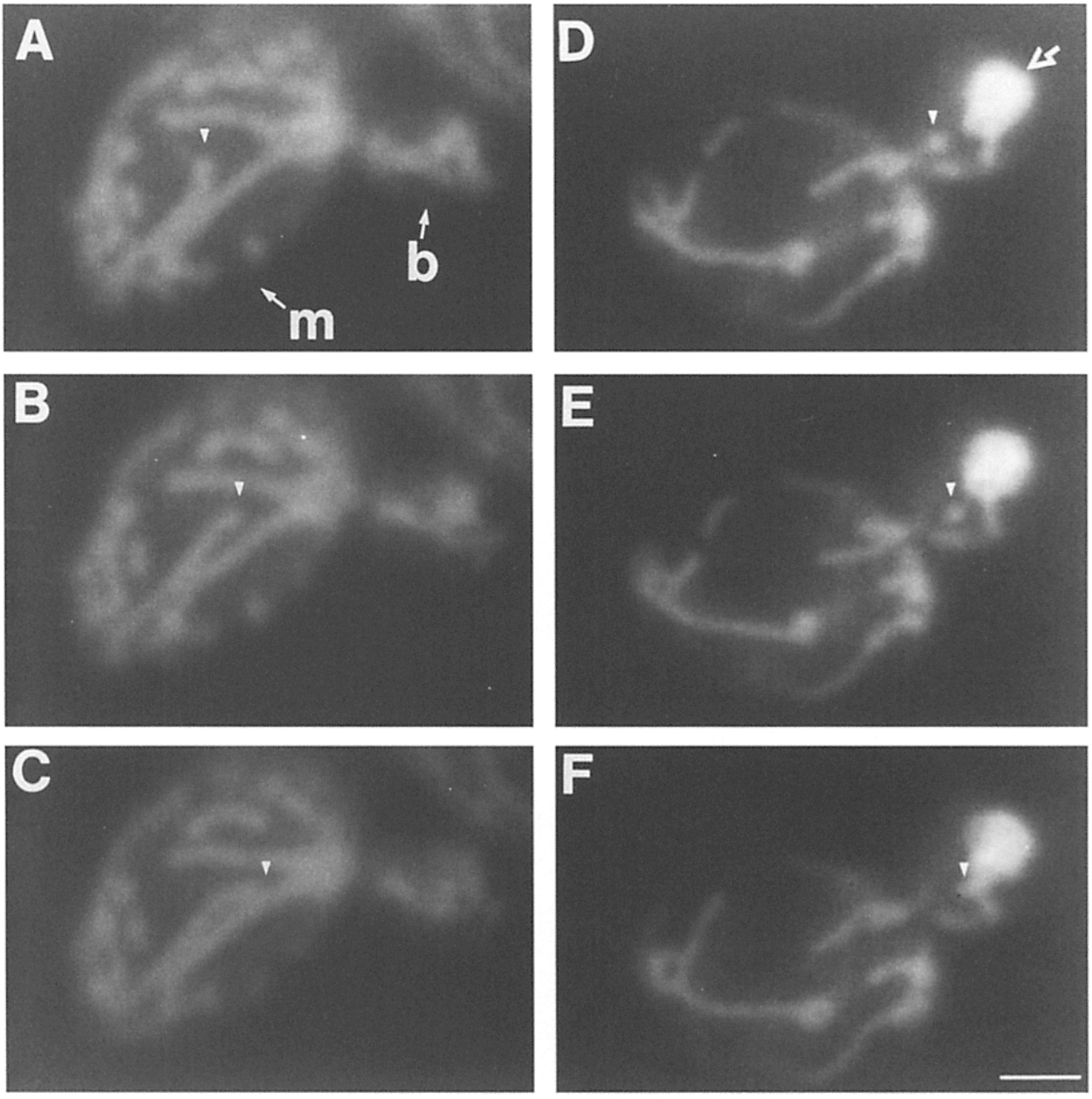

Figure 1. Mitochondrial movements in mitotic yeast are linear and polarized. Wild-type yeast (MSY106) were grown to mid-log phase in rich, glucose-based medium (YPD) at 22°C. Cells were stained by incubation with the membrane potential sensing dye $DiOC_6$. Thereafter, cells were concentrated by low speed centrifugation, resuspended in YPD, and visualized by time-lapse fluorescence microscopy at 30°C. Mitochondria are resolved as brightly labeled spheres and long tubules. *A–C* and *D–F* are consecutive still frames collected at 20-s intervals which show polarized mitochondrial movement in mitotic yeast. Within each set of still frames, arrowheads mark the position of a moving mitochondrion. The arrow in panel *D* points to mitochondria accumulating at the bud tip. *m*, mother cell; *b*, bud. Bar, 1.5 μm.

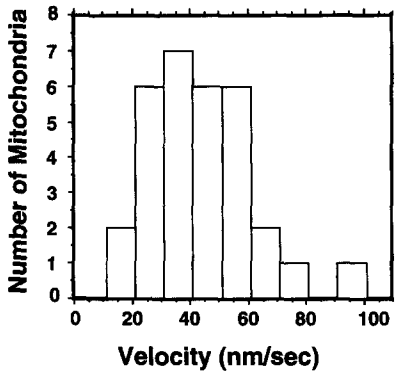

Figure 2. Frequency distribution of mitochondrial velocities in vivo. Velocities of mitochondrial movement were determined by measuring the change in position of the leading tip of each motile organelle as a function of time, as described in Materials and Methods. The histogram shows frequencies of measured velocities from six experiments.

The extent of mitochondrial motility varies in different regions of budding yeast and is not significantly affected by progression through the cell cycle. Budding cells were divided into four regions: (*a*) the peripheral region in the mother distal to the site of bud emergence, (*b*) the central region of the mother, (*c*) the bud and bud neck region, and (*d*) the bud tip (Table II). High levels of mitochondrial motility occur in the central region of the mother cell, bud neck, and bud. In contrast, significantly lower levels of mitochondrial motility occur in the peripheral region of the mother cell distal to the bud and in the bud tip. Finally, the region-specific pattern of mitochondrial motility does not change over the S, G_2, and M phases of the cell cycle as indicated by bud size (Table II).

Mitochondrial Movements in Actin and Myosin Mutants

Mitochondrial inheritance is compromised in yeast bearing temperature-sensitive mutations in the *ACT1* gene. To determine whether this defect is the result of impaired organelle movement, we investigated mitochondrial movement in cells bearing *act1-3* and *act1-133* alleles after short-term shift to semipermissive temperature. Mitochondria in *act1-133* and *act1-3* cells are not tubular, nor are they aligned in the center of the mother cell. Instead, mitochondria are resolved as randomly positioned aggregates (Drubin et al., 1993; Lazzarino et al., 1994). Time-lapse sequences of $DiOC_6$- or MitoTracker-stained cells indicate that mitochondrial movement is severely impaired in these mutants after short-term shift to semipermissive or restrictive temperatures (Table III). In all but one of the *act1-3* and *act1-133* mutant cells recorded ($n = 70$) all mitochondrial structures were static. One cell contained a mitochondrion that displayed very short oscillations which did not alter its position significantly. Long-distance, polarized mitochondrial movements were not observed.

These studies suggest a role for the actin cytoskeleton in control of mitochondrial spatial arrangement, movement and inheritance. Myosins have been implicated in actin-dependent organelle motility. Therefore, we investigated mitochondrial arrangement and movement in strains bearing single deletion mutations in the *MYO1, MYO3,* or *MYO4* genes or a temperature-sensitive mutation in the *MYO2* gene. *MYO2* and *MYO4* encode type V unconventional myosins. Since myosins of the same type may perform overlapping functions, we also examined mitochondrial movement in a *myo2, myo4* double mutant. Deletion of *myo1, myo3,* or *myo4* has no significant effect on mitochondrial morphology or motility. In all three strains, mitochondrial movements are long distance and polarized and have an average velocity similar to that of mitochondria in wild-type cells (Table III).

The *myo2-66* allele is a temperature-sensitive mutation which disrupts vesicle transport, cell polarization, and cell growth. After 30 min of shift to restrictive temperatures, *myo2* mutants display vesicle accumulation and low levels

Table II. Region-Specific Differential Movement of Mitochondria in Dividing Yeast

	Percent motile mitochondria			
Bud size	Periphery	Central	Bud neck	Bud tip
Small	20	69	73	–
Medium	21	61	79	0
Large	29	55	66	0
All bud sizes	21	66	76	0

Cells bearing small (1–2.5 μm), medium (2.6–3.5 μm) and large (3.6–4.5 μm) sized buds are in the S, G_2, and M phases of the cell cycle, respectively (Pringle and Hartwell, 1981). The percentage of organelles moving in different regions of dividing cells was determined as a function of bud size ($n = 80$ cells). Motile mitochondria were defined as described in Materials and Methods. The high density of accumulated mitochondria at the bud tip precludes resolution of individual organelles. Therefore, we assumed that each mitochondrial accumulation in the bud tip consists of one organelle, and defined movement as translocation from the bud toward the mother cell.

Table III. The Velocity of Mitochondrial Movement in Actin and Myosin Mutants

Strain		Temperature (°C)	Velocity
			nm/sec
MSY106	*ACT1*	30	49 ± 21
DDY437	*act1-133* ts	30	0
MSY202	*act1-3* ts	30	0
DBY745	*MYO1*	30	46 ± 12
BN4	*myo1Δ*	30	43 ± 15
SLY87	*MYO2*	22	37 ± 17
		37	48 ± 25
SLY88	*myo2-66* ts	22	30 ± 8
		37	36 ± 10
CRY3	*MYO3*	30	30 ± 12
HGA1	*myo3Δ*	30	36 ± 16
22AB	*MYO4*	30	37 ± 7
MYO4ΔU5	*myo4Δ*	30	36 ± 13
VSY30	*myo2-66, myo4Δ* ts	22	40 ± 17
		37	37 ± 14

Cells were grown to mid-log phase in YPD and stained with $DiOC_6$ or MitoTracker as described in Materials and Methods. *myo1, myo3,* and *myo4* and their respective parental strains were grown and visualized using $DiOC_6$ at 30°C. Actin mutants and wild-type controls were grown at 22°C, stained with MitoTracker and visualized at semipermissive temperatures (30°C) 30 min after temperature shift. The *myo2* and *myo2, myo4* mutant strains were grown at 22°C, shifted to 22°C or 37°C and visualized using $DiOC_6$, 30, 45, 60, and 120 min after temperature shift. The velocities shown were obtained 30 min after temperature shift. Mitochondrial distribution and motility were analyzed by time-lapse fluorescence microscopy and velocities were determined as described in Materials and Methods. Each velocity represents the average of 20–100 measurements.

of actin mislocalization (Johnston et al., 1991; Govindan et al., 1995). Under these conditions, we find that wild-type cells and *myo2* mutants display normal, polarized mitochondrial motility. The *myo2, myo4* double mutant is phenotypically similar to the *myo2* mutant in actin structure and mitochondrial distribution and movement. Prolonged temperature shift results in mitochondrial aggregation and loss of mitochondrial motility in both *myo2* and *myo2, myo4* mutants. However, since these changes correlate with severe loss of polarization of the actin cytoskeleton, we attribute these defects to indirect effects on actin structures rather than direct effects on myosin activity.

Identification of Actin-dependent Motor Activity on Isolated Mitochondria

A modification of the Kron and Spudich sliding filament assay (1986) was used to study actin-based motor activity on yeast mitochondria. We find that rhodamine-phalloidin–labeled yeast actin filaments bind to mitochondria immobilized on a microscope flow cell in the absence of ATP. Under these ATP-depleted conditions, we do not detect any microfilament sliding on immobilized mitochondria. In contrast, addition of low levels of ATP (10 μM) and an ATP regeneration system results in unidirectional sliding of microfilaments on the surface of mitochondria (Fig. 3). Although the sliding activity varies with different mitochondrial preparations, up to 35% of the bound actin filaments display ATP-dependent sliding. In all cases, sliding of microfilaments colocalizes with $DiOC_6$-stained mitochondria and occurs parallel to the long axis of the filament with one end of the filament leading. The average velocity of microfilament sliding in the presence of 10 μM ATP is 22 ± 10 nm/sec. The frequency distribution of filament sliding velocities is shown in Fig. 4.

ATP titration reveals no significant microfilament sliding at concentrations equal to or below 100 nM ATP (Fig. 5). With 500 nM–5 μM ATP, we observe a linear increase in microfilament sliding velocities from 15–25 nm/sec. Sliding velocities reach a plateau above 5 μM ATP: there is no significant difference in the sliding velocities at 5–100 μM ATP as determined by the Student's *t* test and analysis of variances. The maximum velocity of microfilament sliding at ATP concentrations of 5–100 μM is 23 ± 11 nm/sec. At high levels of ATP (500 μM–2 mM), we do not detect microfilament sliding. Rather, bound F-actin detaches from immobilized mitochondria. Although the extent of ATP sensitivity of this interaction varies in different organelle preparations, we find that an average of 40% of filaments detach from the mitochondrial surface in the presence of 2 mM ATP.

Previous studies indicate that cytoskeleton-dependent

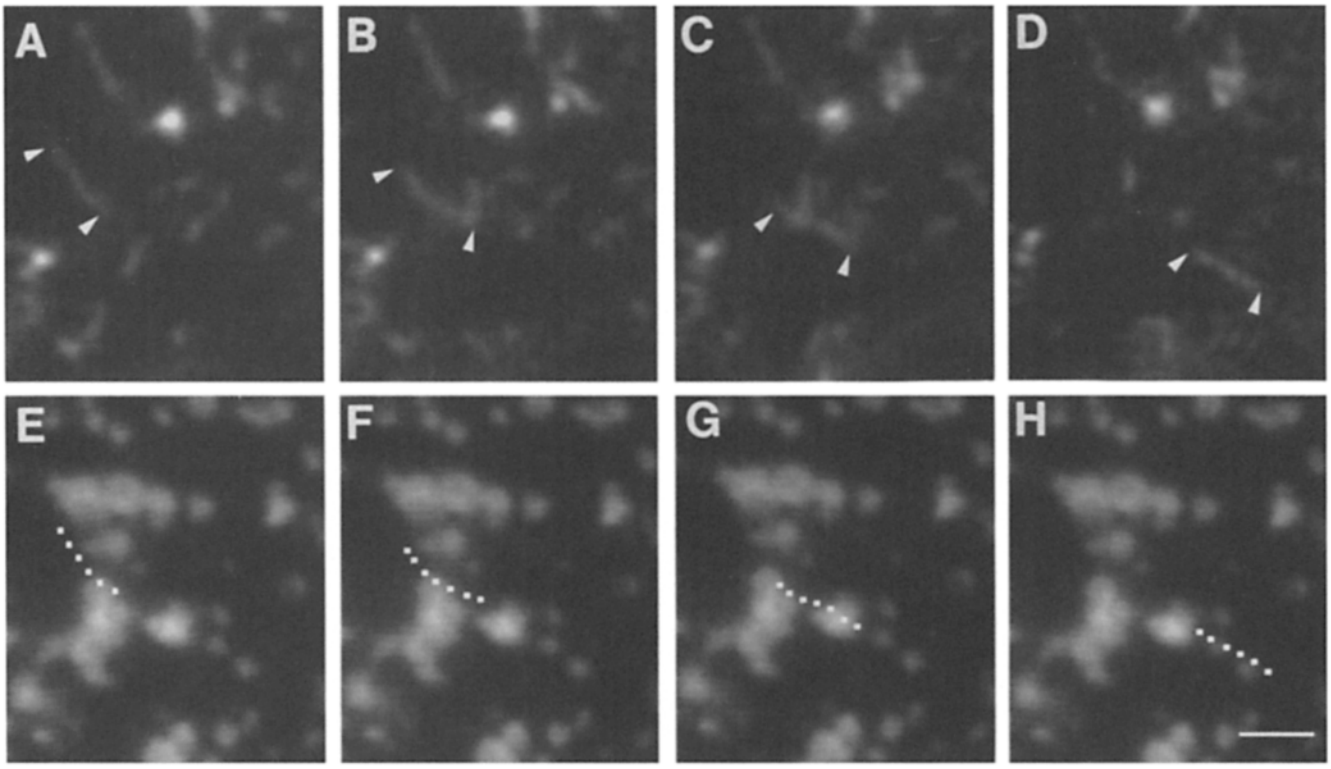

Figure 3. Actin-based ATP-dependent motor activity on isolated mitochondria. Isolated yeast mitochondria were stained with $DiOC_6$ and immobilized within a microscope flow cell. The flow cell was washed by perfusion with BSA-containing AB buffer and rhodamine phalloidin–labeled yeast actin filaments were introduced. After washes to remove nonspecifically bound material, low levels of ATP (10 μM) and an ATP-regenerating system were added. The positions of $DiOC_6$-stained mitochondria and rhodamine-labeled F-actin were determined by time-lapse fluorescence microscopy as described in Materials and Methods. (*A–D*) Consecutive images of rhodamine phalloidin–labeled F-actin at 0, 60, 140, and 260 s after addition of ATP. Arrows point to the ends of a filament moving from the left center to the lower right of the field. (*E–H*) $DiOC_6$-stained mitochondria underlying the moving filament. Tracings in *E–H* mark the position of the filament as it slides along the surface of the immobilized organelles. Bar, 1 μm.

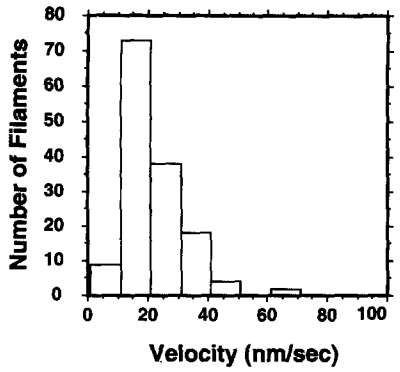

Figure 4. Frequency distribution of microfilament sliding velocities. The velocity of microfilament sliding in the presence of 10 μM ATP was determined by measuring the translocation distance of the leading tip of a moving microfilament as a function of time for 94 filaments in four experiments. Velocities were determined only for filaments that colocalized with $DiOC_6$-stained mitochondria. The average filament sliding velocity was 22 ± 10 nm/sec.

motor molecules require ATP hydrolysis. We find that the nonhydrolyzable ATP analog AMP-PNP will not support microfilament sliding at 10 or 100 μM, concentrations 10–100 times higher than the minimum ATP concentration necessary to support movement (Fig. 5). Thus, mitochondrial motor activity, like that of other cytoskeleton-dependent motors, requires ATP and ATP hydrolysis.

Mitochondrial Outer Membrane Protein(s) Show ATP-sensitive Binding to F-Actin

To examine the submitochondrial localization of this activity, right-side-out sealed yeast mitochondrial outer membrane (OM) vesicles (Riezman et al., 1983) were immobilized in a flow cell and incubated with actin filaments (Fig. 6). Indirect immunofluorescence using antibodies against outer membrane marker proteins confirmed that OM vesicles adhere to the nitrocellulose-coated coverslip. F-actin binding to OM vesicles is stable through several buffer washes, but is sensitive to washes of buffer containing 2 mM ATP. 65–70% of filaments detached from the OM-coated surface after treatment with 2 mM ATP. Thus, mitochondrial outer membrane vesicles contain ATP-sensitive actin-binding activity resembling that observed in intact mitochondria. These findings suggest that the motor activity is localized on the outer leaflet of the mitochondrial outer membrane. Consistent with this, we observe that mild trypsin treatment of mitochondrial outer membrane vesicles results in 95% inhibition of F-actin binding. Thus, mitochondria-microfilament binding is mediated by a protein or proteins on the mitochondrial outer membrane.

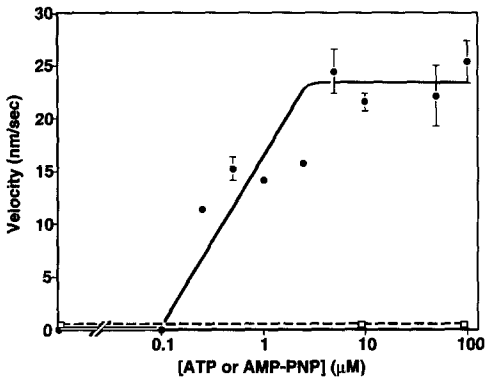

Figure 5. The mitochondrial motor activity is ATP concentration-dependent and requires ATP hydrolysis. Rhodamine-phalloidin–labeled microfilaments were bound to immobilized mitochondria as for Fig. 3. After washes to remove unbound material, AB buffer containing 100 nM–100 μM ATP and an ATP-regenerating system (*closed circles*) or AMP-PNP (*white squares*) was added to separate flow cells. Microfilament sliding was recorded by time-lapse imaging. The average velocity of microfilament sliding was determined as described in Materials and Methods. Each point in the curve represents the mean of >50 filament velocities. Bars show standard error for each measurement.

Discussion

Using time-lapse video microscopy and membrane potential sensing dyes, we have resolved three distinct mitochondrial motility events during mitochondrial inheritance in dividing cells: (*1*) transfer of mitochondria from the mother cell to the developing bud, (*2*) retention of newly inherited mitochondria in the bud tip, and (*3*) retention of some mitochondria within the mother cell. Each of these events appears to result from regulated, directed organelle movements. First, tubular mitochondria in the central region of the mother cell display polarized, linear movement into developing daughter cells. Second, retention of mitochondria within the bud and within the mother cell may be achieved by localized downregulation of mitochondrial movements. These immobilization and polarized mobilization events contribute to the efficiency and pattern of mitochondrial inheritance.

In budding yeast, cell cycle–dependent actin rearrangements result in deposition of actin cables extending from the bud to deep within the mother cell. Mitochondria colocalize with these actin cables. In addition, mutants bearing temperature-sensitive lethal mutations in the *ACT1* gene display defects in mitochondrial spatial arrangement and inheritance (Drubin et al., 1993; Lazzarino et al., 1994). We find that mitochondrial movements are also impaired in vegetative actin mutants. Together, these findings indicate that mitochondria-actin interactions are functionally significant and that one consequence of these interactions is control of mitochondrial location and movement during inheritance.

One of the mutants used (*act1-133*) contains two amino acid substitutions at positions 24 and 25, residues within the myosin-binding site of actin. Microfilament sliding assays using *Dictyostelium* F-actin bearing mutations at the same residues reveal that the mutant F-actin will bind, but will not slide on, heavy meromyosin–coated surfaces. These studies implicate residues 24 and 25 in ATP-driven sliding and force generation (Johara et al., 1993). Our findings that (*a*) mitochondria in the *act1-133* mutant do not display any significant movement, and (*b*) mitochondria contain an ATP-sensitive F-actin–binding activity, implicate actin as a track for directed mitochondrial movement. To explore this issue, we studied actin-dependent mitochondrial movement in cell-free systems. Microfilament sliding assays indicate that mitochondria contain an actin-dependent, ATP-driven motor activity. The maximum ve-

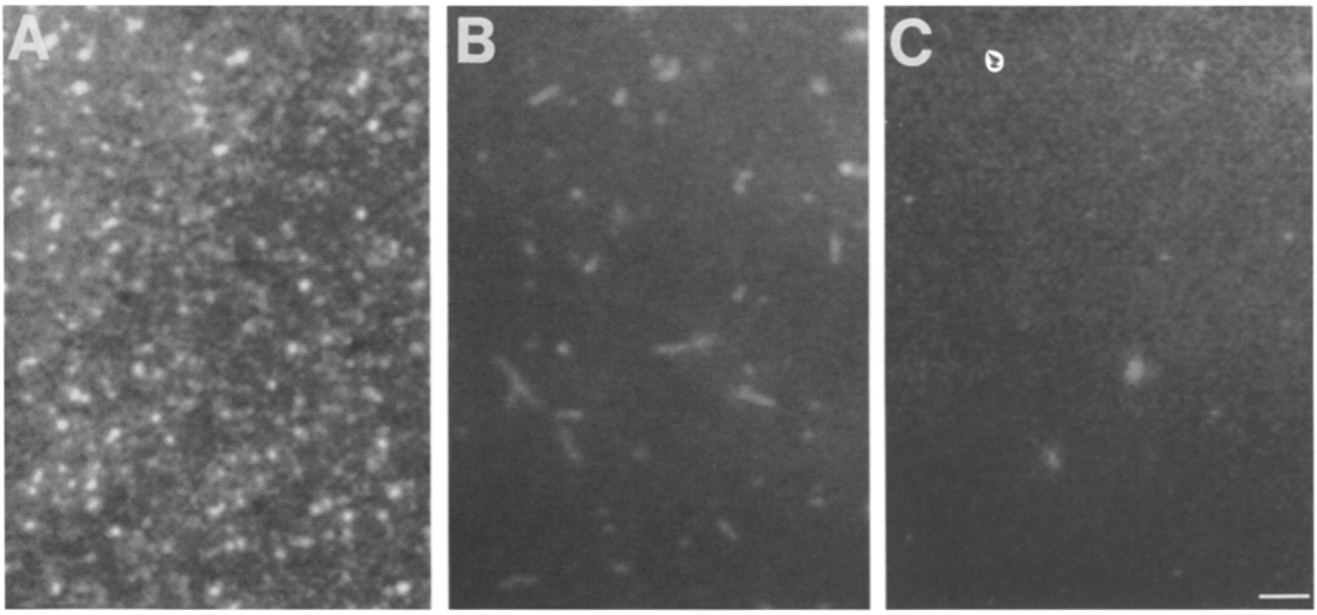

Figure 6. ATP-sensitive binding of F-actin to mitochondrial outer membrane vesicles. Mitochondrial outer membrane vesicles were immobilized in a microscope flow cell and incubated with rhodamine-phalloidin actin filaments as for Fig. 3. After washes to remove nonspecifically bound material, the flow cell was perfused with AB buffer containing 2 mM ATP and an ATP-regenerating system. Filament binding to immobilized mitochondrial outer membranes before (*B*) and after (*C*) ATP treatment was determined by fluorescence imaging. We observe that short and medium length actin filaments (0.25–1.2 μm) bind to OM vesicles and that ATP treatment releases the bound F-actin. In a parallel experiment, immobilized outer membrane vesicles were decorated with an antibody raised against a mitochondrial outer membrane marker protein (Mas70p) and antigen-antibody complexes were detected using FITC-coupled secondary antibody (*A*). Bar, 1 μm.

locity of microfilament sliding on the surface of mitochondria is 23 ± 11 nm/sec. The velocity of this microfilament sliding is low compared to that produced by myosins (i.e., rabbit skeletal muscle myosin II, 3–4 μm/sec; *Dictyostelium* myosin II, 1–2 μm/sec; turkey smooth muscle myosin II, 237 nm/sec; human platelet cytoplasmic myosin, 54 nm/sec)(Kron and Spudich, 1986; Umemoto and Sellers, 1990). However, the peak and mean velocities for in vitro motility are similar to those of mitochondrial movement in mitotic yeast. Therefore, mitochondria-driven microfilament sliding in vitro accurately reflects mitochondrial motility in living cells. This velocity is sufficient for transfer of mitochondria from mother to daughter cell (given the 3 μm diameter of a haploid yeast), within the period of a typical yeast cell cycle (90–120 min).

Previous studies indicate that ATP-sensitive actin-binding activity is enriched upon purification of mitochondria by differential and isopycnic centrifugation, and is blocked by protease digestion of mitochondrial surface proteins (Lazzarino et al., 1994). This finding suggests that ATP-sensitive actin-binding activity is not due to contaminating membranes in the mitochondrial preparation. Submitochondrial fractionation studies were used to further localize the mitochondrial actin-binding activity. We find that: (*a*) right-side-out sealed outer membrane vesicles display ATP-sensitive actin-binding activity, and (*b*) protease treatment of mitochondrial outer membrane vesicles abolishes F-actin binding. Thus, this ATP-sensitive motor activity is localized to the outer leaflet of the mitochondrial outer membrane. Finally, since microfilament sliding on immobilized mitochondria does not require cytosolic extracts, it appears that all of the elements required for mitochondrial motor activity are present on the mitochondrial surface.

The only known actin-dependent motor molecules are members of the myosin superfamily. Our evidence suggests that the mitochondrial motor activity has properties similar to those of myosins. First, saturation of myosin-binding sites on F-actin blocks binding of mitochondria to F-actin (Lazzarino et al., 1994). In addition, using the microfilament sliding assay, we observe that the mitochondrial motor drives microfilament sliding parallel to the long axis of F-actin. This motor requires ATP hydrolysis: a nonhydrolyzable ATP analog will not support movement. Finally, myosin activity requires critical concentrations of Mg^{+2}-ATP (Weber, 1969; Reuben et al., 1971). The concentration of ATP required for contraction of skinned muscle fibers is similar to that required for ATP-sensitive actin-mitochondrial interactions. Although the mitochondrial motor activity resembles that of myosin, our findings indicate that this activity is not encoded exclusively by any of the known myosin genes: the polarity, regulation, and velocity of mitochondrial movement are not directly affected in *myo1, myo2, myo3, myo4*, or *myo2, myo4* mutants.

Collectively, our findings indicate that mitochondrial inheritance during yeast cell division is achieved through polarized, regulated mitochondrial movements. These organelle motility events appear to be mediated by direct interactions between mitochondria and the actin cytoskeleton, and driven by an actin-dependent motor activity on the mitochondrial outer membrane. The mitochondrial motor described in these studies represents the first documented case of an actin-dependent motor activity identi-

fied in a defined organelle population. In addition, our studies indicate that mitochondrial inheritance is linked to the cell polarization machinery required for asymmetric yeast cell growth: the tracks for mitotic mitochondrial movement appear to be actin cables that extend from the bud into the mother cell. Current efforts are directed towards purifying and cloning the mitochondrial motor, and identifying the mechanisms that regulate mitochondrial motor activity.

We would like to thank S. Atkinson, T. Pollard, and D. Lazzarino for invaluable assistance with the microfilament sliding assay; S. Brown, D. Drubin, H. Goodson, J. Rodriguez-Medina, and J. Spudich for yeast strains; P. Brandt, R. Liem, I. Boldogh, and M. Smith for support and critical comments on the manuscript; K. Rosa for photography; H. O'Sullivan and N. Vojtov for expert technical assistance.

This work was supported by a predoctoral National Research Service Award (5 F31 GM15644) to V. Simon; a National Science Foundation predoctoral fellowship to T. Swayne; as well as a Research grant (RO1 GM45735) from the National Institutes of Health, a Grant-in-aid Award (AHA CU50706601) from the American Heart Association, and a Basil O'Connor Starter Scholar Research Award (MDBDF #5-FY92-1143) from the March of Dimes.

Received for publication 19 December 1994 and in revised form 21 April 1995.

References

Adams, A. E. M., and J. R. Pringle. 1984. Relationship of actin and tubulin distribution to bud growth in wild-type and morphogenetic-mutant *Saccharomyces cerevisiae*. *J. Cell Biol.* 98:934–945.

Adams, R. J., and T. D. Pollard. 1986. Propulsion of organelles isolated from *Acanthamoeba* along actin filaments by myosin-I. *Nature (Lond.).* 322:754–756.

Adams, R. J., and T. D. Pollard. 1989. Membrane-bound myosin-I provides new mechanisms in cell motility. *Cell Motil. Cytoskeleton.* 14:178–182.

Albanesi, J. P., J. Fujisaki, J. A. Hammer, III, E. D. Korn, R. Jones, and M. P. Sheetz. 1985. Monomeric *Acanthamoeba* myosins-I support movement in vitro. *J. Biol. Chem.* 98:934–945.

Brockerhoff, S. E., R. C. Stevens, and T. N. Davis. 1994. The unconventional myosin, Myo2p, is a calmodulin target at sites of cell growth in *Saccharomyces cerevisiae*. *J. Cell Biol.* 124:315–323.

Chen, L. B. 1989. Fluorescent labeling of mitochondria. *Methods Cell Biol.* 29: 103–123.

Criddle, R. S., and G. Schatz. 1969. Promitochondria of anaerobically grown yeast. I. Isolation and biochemical properties. *Biochemistry.* 8:322–334.

Drubin, D. G., K. G. Miller, and K. F. Wertman. 1993. Actin structure and function: roles in mitochondrial organization and morphogenesis in budding yeast and identification of the phalloidin binding site. *Mol. Biol. Cell.* 4: 1277–1294.

Fath, K. R., and D. R. Burgess. 1993. Golgi-derived vesicles from developing epithelial cells bind actin filaments and possess myosin-I as a cytoplasmically oriented peripheral membrane protein. *J. Cell Biol.* 120:117–127.

Glick, B. S., and L. A. Pon. 1995. Isolation of highly purified yeast mitochondria. *Methods Enzymol.* 260:213–223.

Goodson, H. V., and J. A. Spudich. 1995. Identification and molecular characterization of a yeast myosin I. *Cell Motil. Cytoskeleton.* 30:73–84.

Govindan, B., R. Bowser, and P. Novick. 1995. The role of Myo2, a yeast class V myosin, in vesicular transport. *J. Cell Biol.* 128:1055–1068.

Grolig, F., R. E. Williamson, J. Parke, C. Miller, and B. H. Anderton. 1988. Myosin and Ca^{+2} -sensitive streaming in the alga *Chara:* detection of two polypeptides reacting with a monoclonal anti-myosin and their localization in the streaming endoplasm. *Eur. J. Cell Biol.* 47:22–31.

Haarer, B. K., A. Petzold, S. H. Lillie, and S. S. Brown. 1994. Identification of *MYO4*, a second class V myosin gene in yeast. *J. Cell Sci.* 107:1055–1064.

Hegmann, T. E., D. L. Schulte, J. L. Lin, and J. J. Lin. 1990. Inhibition of intracellular granule movement by microinjection of monoclonal antibodies against caldesmon. *Cell Motil. Cytoskeleton.* 20:109–120.

Huffaker, T. C., J. H. Thomas, and D. Botstein. 1988. Diverse effects of β-tubulin mutations on microtubule formation and function. *J. Cell Biol.* 106:1997–2010.

Jacobs, C. W., A. E. M. Adams, P. J. Szaniszlo, and J. R. Pringle. 1988. Functions of microtubules in the *Saccharomyces cerevisiae* cell cycle. *J. Cell Biol.* 107:1409–1426.

Johara, M., Y. Y. Toyoshima, A. Ishijima, H. Kojima, T. Yanagida, and K. Sutoh. 1993. Charge-reversion mutagenesis of *Dictyostelium* actin to map the surface recognized by myosin during ATP-driven sliding motion. *Proc. Natl. Acad. Sci. USA.* 90:2127–2131.

Johnston, G. C., J. A. Prendergast, and R. A. Singer. 1991. The *Saccharomyces cerevisiae MYO2* gene encodes an essential myosin for vectorial transport of vesicles. *J. Cell Biol.* 113:539–551.

Kabsch, W., H. G. Mannherz, D. Suck, E. F. Pai, and K. C. Holmes. 1990. Atomic structure of the actin:DNase I complex. *Nature (Lond.).* 347:37–44.

Kachar, B. 1985. Direct visualization of organelle movement along actin filaments dissociated from Characean algae. *Science (Wash. DC).* 227:1355–1357.

Kachar, B., and T. S. Reese. 1988. The mechanism of cytoplasmic streaming in Characean algal cells: sliding of endoplasmic reticulum along actin filaments. *J. Cell Biol.* 106:1545–1552.

Kilmartin, J. V., and A. E. M. Adams. 1984. Structural rearrangements of tubulin and actin during the cell cycle of the yeast *Saccharomyces*. *J. Cell Biol.* 98: 922–933.

Koning, A. J., P. K. Lum, J. M. Williams, and R. Wright. 1993. $DiOC_6$ staining reveals organelle structure and dynamics in living yeast cells. *Cell Motil. Cytoskeleton.* 25:111-128.

Kron, S. J., and J. Spudich. 1986. Fluorescent actin filaments move on myosin fixed to a glass surface. *Proc. Natl. Acad. Sci. USA.* 83:6272–6276.

Kübler, E., and H. Riezman. 1993. Actin and fimbrin are required for the internalization step of endocytosis in yeast. *EMBO (Eur. Mol. Biol. Organ.) J.* 12: 2855–2862.

Kuznetsov, S. A., G. M. Langford, and D. G. Weiss. 1992. Actin-dependent organelle movement in squid axoplasm. *Nature (Lond.).* 356:722–725.

Lazzarino, D. A., I. Boldogh, M. G. Smith, J. Rosand, and L. A. Pon. 1994. ATP-sensitive, reversible actin binding activity in isolated yeast mitochondria. *Mol. Biol. Cell.* 5:807–818.

Lillie, S. H., and S. S. Brown. 1994. Immunofluorescence localization of the unconventional myosin, Myo2p, and the putative kinesin-related protein, Smy1p, to the same regions of polarized growth in *Saccharomyces cerevisiae*. *J. Cell Biol*. 125:825–842.

Mulholland, J., D. Preuss, A. Moon, A. Wong, D. Drubin, and D. Botstein. 1994. Ultrastructure of the yeast actin cytoskeleton and its association with the plasma membrane. *J. Cell Biol.* 125:381–391.

Novick, P., and D. Botstein. 1985. Phenotypic analysis of temperature-sensitive yeast actin mutants. *Cell.* 40:405–416.

Palmer, R. E., D. S. Sullivan, T. Huffaker, and D. Koshland. 1992. Role of astral microtubules and actin in spindle orientation and migration in the budding yeast, *Saccharomyces cerevisiae*. *J. Cell Biol.* 119:583–593.

Prendergast, J. A., L. E. Murray, A. Rowley, D. R. Carruthers, R. A. Singer, and G. C. Johnston. 1990. Size selection identifies new genes that regulate *Saccharomyces cerevisiae* cell proliferation. *Genetics.* 124:81–90.

Pringle, J. R., and L. H. Hartwell. 1981. The *Saccharomyces cerevisiae* cell cycle. *In* The Molecular Biology of the Yeast *Saccharomyces*: Life Cycle and Inheritance. J. N. Strathern, E. W. Jones, and J. R. Broach, editors. Cold Spring Harbor Laboratory, Cold Spring Harbor, New York. 97–142.

Rayment, I., H. M. Holden, M. Whittaker, C. B. Yohn, M. Lorenz, K. C. Holmes, and R. A. Milligan. 1993. Structure of the actin-myosin complex and its implications for muscle contraction. *Science (Wash. DC).* 261:58–65.

Read, E. B., H. H. Okamura, and D. G. Drubin. 1992. Actin- and tubulin-dependent functions during *Saccharomyces cerevisiae* mating projection formation. *Mol. Biol. Cell.* 3: 429–444.

Reuben, J. P., P. W. Brandt, M. Berman, and H. Grundfest. 1971. Regulation of tension in the skinned crayfish muscle fiber. *J. Gen. Physiol.* 57:385–407.

Riezman, H., R. Hay, S. Gasser, G. Daum, G. Schneider, C. Witte, and G. Schatz. 1983. The outer membrane of yeast mitochondria: isolation of outside-out sealed vesicles. *EMBO (Eur. Mol. Biol. Organ.) J.* 2:1105–1111.

Rodriguez, J. R., and B. Paterson. 1990. Yeast myosin heavy chain mutant: maintenance of the cell type specific budding pattern and the normal deposition of chitin and cell wall components requires an intact myosin heavy chain gene. *Cell Motil. Cytoskeleton.* 17:301–308.

Schatz, G., and J. Saltzgaber. 1969. Protein synthesis by yeast promitochondria *in vivo*. *Biochem. Biophys. Res. Commun.* 37:996–1001.

Schröder, R. R., D. J. Manstein, W. Jahn, H. Holden, I. Rayment, K. C. Holmes, and J. A. Spudich. 1993. Three-dimensional atomic model of F-actin decorated with *Dictyostelium* myosin S1. *Nature (Lond.).* 364:171–174.

Sheetz, M. P., and J. A. Spudich. 1983. Movement of myosin-coated fluorescent beads on actin cables *in vitro*. *Nature (Lond.).* 303:31-35.

Sherman, F. 1991. Getting started with yeast. *Methods Enzymol.* 194:3–37.

Shortle, D., P. Novick, and D. Botstein. 1984. Construction and genetic characterization of temperature-sensitive mutant alleles of the yeast actin gene. *Proc. Natl. Acad. Sci. USA.* 81:4889–4893.

Stevens, B. 1981. Mitochondrial structure. *In* The Molecular Biology of the Yeast *Saccharomyces*: Life Cycle and Inheritance. J. N. Strathern, E. W. Jones, and J. R. Broach, editors. Cold Spring Harbor Laboratory, Cold Spring Harbor, New York. 471–488.

Umemoto, S., and J. R. Sellers. 1990. Characterization of *in vitro* motility assays using smooth muscle and cytoplasmic myosins. *J. Biol. Chem.* 265:14864–14869.

Watts, F. Z., G. Shiels, and E. Orr. 1987. The yeast *MYO1* gene encoding a myosin-like protein required for cell division. *EMBO (Eur. Mol. Biol. Organ.) J.* 6:3499–3505.

Weber, A. 1969. Parallel response of myofibrillar contraction and relaxation to

four different nucleoside triphosphates. *J. Gen. Physiol.* 53:781–791.
Wertman, K. F., D. G. Drubin, and D. Botstein. 1992. Systematic mutational analysis of the yeast *ACT1* gene. *Genetics.* 132:1–14.
Wessels, D., N. A. Schroeder, E. Voss, A. L. Hall, J. Condeelis, and D. R. Soll. 1989. cAMP-mediated inhibition of intracellular particle movement and actin reorganization in *Dictyostelium. J. Cell Biol.* 109:2841–2851.
Wessels, D., and D. R. Soll. 1990. Myosin II heavy chain null mutant of *Dictyostelium* exhibits defective intracellular particle movement. *J. Cell Biol.* 111: 1137–1148.
Whitaker, J. E., P. L. Moore, R. P. Haugland, and R. P. Haugland. 1991. Dihydrotetramethylrosamine: a long wavelength, fluorogenic peroxidase substrate evaluated *in vitro* and in a model phagocyte. *Biochem. Biophys. Res. Commun.* 175:387–393.